Synthetic and Systems Biotechnology 1 (2016) 47–55

Contents lists available at ScienceDirect

Synthetic and Systems Biotechnology

journal homepage: keaipublishing.com/synbio

Systematic development of biomass overproducing *Scheffersomyces stipitis* for high-cell-density fermentations

Pornkamol Unrean *, Sukanya Jeennor, Kobkul Laoteng

National Center for Genetic Engineering and Biotechnology (BIOTEC), National Science and Technology Development Agency (NSTDA), 113 Thailand Science Park Phahonyothin Road, Klong Nueng, Klong Luang, Pathum Thani 12120, Thailand

ARTICLE INFO

Article history:
Received 13 December 2015
Received in revised form 5 January 2016
Accepted 10 January 2016
Available online

Keywords:
Scheffersomyces stipites
Efficient strain design
Biomass production
Systems metabolic engineering
Metabolic evolution

ABSTRACT

The development of economically feasible bio-based process requires efficient cell factories capable of producing the desired product at high titer under high-cell-density fermentation. Herein we present a combinatorial approach based on systems metabolic engineering and metabolic evolution for the development of efficient biomass-producing strain. Systems metabolic engineering guided by flux balance analysis (FBA) was first employed to rationally design mutant strains of *Scheffersomyces stipitis* with high biomass yield. By experimentally implementing these mutations, the biomass yield was improved by 30% in GPD1, 25% in TKL1, 30% in CIT1, and 44% in ZWF1 overexpressed mutants compared to wild-type. These designed mutants were further fine-tuned through metabolic evolution resulting in the maximal biomass yield of 0.49 g-cdw/g-glucose, which matches well with predicted yield phenotype. The constructed mutants are beneficial for biotechnology applications dealing with high cell titer cultivations. This work demonstrates a solid confirmation of systems metabolic engineering in combination with metabolic evolution approach for efficient strain development, which could assist in rapid optimization of cell factory for an economically viable and sustainable bio-based process.

1. Introduction

Achieving sustainable and economical bioprocess requires an efficient cell factory that is able to produce the desired bioproduct at high titer. Such process is mostly accomplished through a high-cell-density cultivation. Thus, high cell yield and high cell titer during fermentation are the primary desired traits for organisms used in the industrial process. Large-scale high cell density cultivation is, however, often limited by the supply of oxygen. Therefore, our work aims at the design and development of cells with the most efficient biomass production under minimized oxygen requirement. Previous attempts of optimizing cells to improve their metabolic capacity have been accomplished through a non-directed method of random mutagenesis followed by screening or engineering of genes in the product synthesis pathway.[1,2] However, these modification strategies may not result in an optimal cell phenotype due to the concerted interplay among metabolic pathways within the cellular network. With increasing information of genome sequence and metabolic pathways, predicting cell phenotype under environmental or genetic perturbations is now possible using a metabolic network model, thereby accelerating the strain development process for biotechnological applications.[3–5] It is, therefore, of particular interest to utilize the systems metabolic engineering approach for the rational design of a biomass overproducing cell.

Scheffersomyces stipitis is a potentially valuable candidate for bioconversion of lignocellulosic residues to fuels and chemicals as it is capable of utilizing various hexose and pentose sugars available in the renewable feedstock.[1,6] The organism also has well-established genetic and metabolic pathway resources. Therefore, as a case demonstration, we utilized systems metabolic engineering together with metabolic evolution for optimizing biomass production in *S. stipitis* with high biomass yield and minimized oxygen requirement. Among the number of existing computation tools for the analysis of cell metabolic network model, flux balance analysis (FBA) has emerged as a powerful tool for analyzing and optimizing cellular metabolism.[7–9] FBA relies on balanced reaction stoichiometry and optimization strategy to identify the optimal flux distribution. Evaluation of flux distribution, which defines the cellular phenotype, permits the rational design of a cell with its functionality limited

* Corresponding author. National Center for Genetic Engineering and Biotechnology (BIOTEC), National Science and Technology Development Agency (NSTDA), 113 Thailand Science Park Phahonyothin Road, Klong Nueng, Klong Luang, Pathum Thani 12120, Thailand. Tel.: 0 2564 6700; fax: 0 2564 6701.
E-mail address: pornkamol.unr@biotec.or.th (P. Unrean).
Peer review under responsibility of KeAi Communications Co., Ltd.

http://dx.doi.org/10.1016/j.synbio.2016.01.006

to efficient pathways. The FBA approach has been applied for improving the production of target metabolites in *Escherichia coli* and *Saccharomyces cerevisiae* such as ethanol, lactic acid, succinic acid, lycopene and etc.[10–13] Yet, no FBA approach has been utilized for the rational design of efficient strain in *S. stipitis*.

We have previously developed a metabolic network model of *S. stipitis* during growth on glucose or xylose.[14] In this work, the model was analyzed by FBA to assess the phenotypic capabilities of this yeast under genetic perturbation and to systematically identify the target of gene overexpression for an efficient conversion of glucose to biomass at high yield. The mutants designed according to the model analysis were experimentally constructed and characterized in comparison with the reference strain. Metabolic evolution strategy was then implemented to fine-tune the metabolism of the constructed mutants for further optimizing biomass production. We reported here the growth performance of these mutant strains, which may potentially be used as a platform host for production of bio-based chemicals from renewable resources under high-cell-density fermentation.

2. Materials and methods

2.1. Yeast strains and plasmids

Wild-type *S. stipitis* CBS6054 (ATCC58785) and its mutant derivatives listed in Table 1 have been used in this study. *E. coli* DH5α (Invitrogen, USA) was used for routine recombinant DNA experiments. pTEF1:mZeo plasmid, kindly provided by Dr. Niran Roongsawang (BIOTEC, Thailand), was used as a backbone for construction of the gene-overexpression plasmids. The construction of pTEF1:mZeo plasmid and its sequence have been described in Puseenam et al.[15] Briefly, the pTEF1:mZeo plasmid was modified from pGAPZαA plasmid (Invitrogen, CA) by replacing native zeocin resistance gene with codon optimized *Sh ble* and replacing *GAP* promoter with constitutive promoter of transcription elongation factor 1 alpha (*TEF1*) from *S. cerevisiae*.

2.2. Construction of overexpressing plasmid

The overexpression plasmids were constructed based on the pTEF1:mZeo plasmid. Four target genes for overexpression are *GPD1* (Glycerol-3-phosphate dehydrogenase, GenBank ID number 4840320); *ZWF1* (Glucose 6-phosphate dehydrogenase, GenBank ID number 4840428); *TKL1* (Transketolase, GenBank ID number 4837370); and *CIT1* (Citrate synthase, GenBank ID number 4841140) as summarized in Supplementary Table S1. Full length cDNAs of target genes were amplified by RT-PCR using high fidelity *Taq* polymerase (Invitrogen, CA) and specified primer pairs which contained appropriate restriction sites at the 5′-end of each primer to facilitate subsequent cloning (Supplementary Table S2). Approximately 50 ng of the first-strand cDNA was used as a template for PCR. The reaction was carried out for 3 min at 94 °C, followed by 35 cycles of 94 °C for 35 s, primer-specific annealing temperature for 40 s, 72 °C for 1.5–3 min and a final extension of 72 °C for 5 min. For *GPD1* and *TKT1* genes, fusion of *TEF1* promoter with *GPD1* or *TKL1* gene by overlap PCR extension technique was performed before sub-cloning. The amplified products were digested and subsequently cloned into appropriated restriction sites of the pTEF1:mZeo vector downstream of the *TEF1* promoter to generate pTEFZ-CIT1, pTEFZ-ZWF1, pTEFZ-GPD1 and pTEFZ-TKL1 plasmids (Table 1). These recombinant plasmids were individually transformed to *S. stipitis* for construction of the four mutant strains with overexpressed genes GPD1, TKT1, CIT1 and ZWF1 based upon non-homologous end joining.

2.3. Yeast transformation and screening of putative overexpressed mutants

Yeast transformation was carried out by lithium acetate (LiAc) and electroporation method.[16] Putative transformants were selected based on their growth on YPD medium supplemented with 100 μg/ml of zeocin. The presence of overexpressed genes in the mutants was confirmed by PCR. DNA fragment containing target gene and partial *AOX1* terminator were amplified using the sense and antisense primers (Supplementary Table S2) corresponding to the 5′ region of target gene (start codon) and *AOX1* terminator in plasmid, respectively. The amplified fragment with expected size and the absence of PCR product are anticipated in the mutants and wild-type, respectively. The constructed mutants containing the overexpressed gene were then tested for their biomass production in comparison with the reference strain.

2.4. Growth medium

YPD (10 g/l yeast extract, 20 g/l peptone and 20 g/l glucose) media and agar plate with zeocin supplement (100 mg/l) was used during strain construction. Defined salt medium (YE) containing 0.1 M potassium phosphate buffer at pH 6.0 (100 ml), 1 g/l yeast extract, 5 g/l $(NH_4)_2SO_4$, 0.1 g/l $CaCl_2$, 0.1 g/l NaCl, 0.5 g/l $MgSO_4$, 1 g/l KH_2PO_4 and 20 g/l glucose was used as a culture media for cell growth studies. Glucose and potassium phosphate buffer solutions were prepared separately, sterilized by autoclave and added to the media prior to use. The solution that contained other components was mixed together and sterilized by autoclave.

Table 1
Strains and plasmids used in this study.

Strains/plasmids	Genotypes	Source
CBS6054	Wild-type	ATCC58785
SJU01	CBS6054 expressing pTEF1:mZeo plasmid containing zeocin^R	This study
SJU02	CBS6054 with GPD1 overexpression	This study
SJU03	CBS6054 with TKL1 overexpression	This study
SJU04	CBS6054 with CIT1 overexpression	This study
SJU05	CBS6054 with ZWF1 overexpression	This study
SJU02E	SJU02 subjected to metabolic evolution through serial dilution experiment for 30 rounds	This study
SJU03E	SJU03 subjected to metabolic evolution through serial dilution experiment for 30 rounds	This study
SJU04E	SJU04 subjected to metabolic evolution through serial dilution experiment for 30 rounds	This study
pTEFZ-GPD1	Integrative plasmid containing *GPD1* under the control of *TEF1* promoter and modified zeocin^R	This study
pTEFZ-TKL1	Integrative plasmid containing *TKL1* under the control of *TEF1* promoter and modified zeocin^R	This study
pTEFZ-CIT1	Integrative plasmid containing *CIT1* under the control of *TEF1* promoter and modified zeocin^R	This study
pTEFZ-ZWF1	Integrative plasmid containing *ZWF1* under the control of *TEF1* promoter and modified zeocin^R	This study

2.5. Batch cultivation

A colony was picked from YPD agar plate and grown in a culture tube containing 4–5 ml of YE media for 16–18 hrs. The culture was then used as inoculum for batch growth kinetic studies carried out in a 250 ml baffled shake flask containing 50 ml of the same media. An initial optical density (OD_{600}) was approximately 0.1–0.2. The cultures were grown in an incubator shaker (Model Innova44, New Brunswick Scientific, USA) at 30 °C with a shaking rate of 100 rpm. Cell samples and supernatants were collected periodically to monitor cell growth, consumed sugar and byproducts.

2.6. Metabolic evolution

Metabolic evolution was carried out by sequentially subculturing of mutant cells in fresh YE media under aerobic condition at 30 °C and a shaking rate of 100 rpm. At each step, the culture was diluted at 1:10 to 1:50 with fresh media after 12–24 hrs intervals to facilitate metabolic evolution with growth-based selection. The evolution process was stopped after 30 rounds of culture transfers. Evolved mutants isolated from selected transfers by plating were measured for their biomass yield in comparison with their parents.

2.7. Analytical techniques

Biomass concentration was measured through optical density at 600 nm (OD_{600}) in 1 cm cuvettes using Spectrophotometer (Biospectrometer, Eppendrof, USA). To determine cell dry weight 3–5 ml of a culture was withdrawn, centrifuged at 5,000 rpm at 4 °C for 5 mins to collect cell pellet. The pellet was washed once with deionized water, added into a pre-weighed tube and dried in an 80 °C oven for 12–24 hrs followed by putting in desiccator for 24 hrs before being subsequently weighed. The following correlation: cell dry weight (g/l) = $0.359 \times OD_{600}$ ($R^2 = 0.96$) was used for estimation of cell dry weight from OD_{600} measurement. Sugar and fermentative byproduct concentration were measured using an HPLC system equipped with a cation exchange column (HPX-87H, Biorad Labs, Hercules, CA) and a refractive index detector (RID-10A). Samples from the culture supernatant were collected, filtered using 0.2 μm sterile filter and stored at –20 °C before analysis. The column was run in an isocratic mode using 5 mM H_2SO_4 mobile phase at 60 °C and a flow rate of 0.6 ml/min for 30 min. A standard curve correlating area to concentration of metabolites was used to determine concentration in the sample.

2.8. Yield and specific rate calculation

Product yield was determined based on gram of product produced per gram of glucose consumed after 24 hrs cultivation, while the overall yield was determined based on total gram of glucose initially added. The specific rate of glucose uptake and secreting byproducts was calculated from curve fitting with the minimized sum of the squared errors to match with the time profiles of measured residual glucose and secreting byproducts during batch growth experiment. Specific growth rate was determined from the slope of a plot of the natural logarithm of the optical density OD_{600} versus time. All parameters including concentration, yield and rate are reported as the mean ± standard deviation from independent duplicate experiments.

2.9. Metabolic model analysis

The metabolic network model of *S. stipitis* grown on glucose was obtained from a previous work.[14] The model represents the core of intermediary metabolism for cell growth, energy synthesis and fermentation. Cell growth is interpreted through the production of biomass from biosynthesis pathways. A linear programming (LP) approach based on MATLAB (Mathworks, Natick, MA, USA) and Mosek optimization toolbox (Mosek ApS, Copenhagen, Denmark) was used for solving stoichiometric mass balance equations to obtain a solution for the unknown fluxes of intracellular and extracellular metabolites,

$$S \cdot q = \begin{bmatrix} b \\ 0 \end{bmatrix} \tag{1}$$

$$q \in \text{irreversible reaction}, q \geq 0$$

where S is an m by n stoichiometric matrix of metabolite m in reaction r_n, q is a column vector composed of net rates of reaction r_n, and b is a vector of accumulation and exchange rates. Maximization of specific growth rate was used as an objective, which is considered a realistic choice given evolutionary pressure on the yeast cell when being cultured under particular growth condition. Nitrogen source, NH_4^+, was assumed to be present in sufficient amount. ATP maintenance requirement was [0, 1] mmol/g-cell·hr, which is a typical value reported for yeast.[17] Gene overexpression simulation was assessed based on the following constraints:

(1) q_{glc}, $q_{O2} = 1$ mmol/g-cell-hr
(2) $q_i = [1.01, 10] \times q_{i,wt}$

where i is the targeted reaction for overexpression and $q_{i,wt}$ is the predicted flux in reference strain.

Biomass yields among different gene overexpression perturbations were compared, and target overexpressed genes resulting in maximum biomass production were determined.

2.10. NADPH and ATP availability calculation

Availability of intracellular redox potential, NADPH, and ATP cofactors used for biomass synthesis is determined principally by accounting for all NADPH and ATP cofactors generated from catabolic reactions within the metabolic network, which are then used for biosynthesis, as follows:

$$\text{NADPH availability (mmol/mmol-glucose)} = \frac{\sum q_{Syn,NADPH,Ri}}{q_{Glc}} \tag{2}$$

$$\text{ATP availability (mmol/mmol-glucose)} = \frac{\sum q_{Syn,ATP,Ri}}{q_{Glc}} \tag{3}$$

where $q_{Syn,NADPH,Ri}$ and $q_{Syn,ATP,Ri}$ are the synthesis rate of NADPH and ATP for each catabolic reaction R_i within the network, respectively. q_{Glc} is the glucose uptake rate (mmol/g-cell·hr).

2.11. Flux control coefficient

The degree of control that a given enzymatic reaction R_i within the metabolic network exerts on biomass production rate, μ, was analyzed based on flux control coefficient (FCC).[18,19] The FCC (C_{Ri}^{μ}) is defined as a relative change in the metabolic flux for biomass synthesis in response to a relative change in enzyme activity, which is directly correlated with the rate of reaction R_i,

$$C_{Ri}^{\mu} = \frac{d \ln \mu}{d \ln R_i} = \frac{\ln \mu^{\max} - \ln \mu}{\ln R_i^{\max} - \ln R_i} \tag{4}$$

where μ and $\mu^{\max}$ represent the flux for biomass synthesis of the mutant and the maximal flux for biomass synthesis predicted by FBA, respectively. R_i and $R_i^{\max}$ represent the individual reaction rate in the mutant and the rate predicted by FBA, respectively. For comparison purposes, all fluxes are normalized with glucose uptake rate.

Reactions exerting elevated flux control by having high flux control coefficient are presumed to be a rate-controlling reaction and could, therefore, be target for engineering to increase metabolic fluxes toward biosynthesis.

3. Results

3.1. Identification of overexpressed gene target

FBA was used to simulate gene overexpression in order to rationally design mutant strain of *S. stipitis* capable of efficiently converting glucose to biomass. Based on the previous model of *S. stipitis*,[14] a predicted maximum yield of 0.49 gram biomass per gram glucose utilized was identified under aerobic growth conditions. The individual enzymatic reaction or in turn its corresponding genes was overexpressed by increasing flux in such reaction (details in the Materials and Methods section). The knowledge of flux distribution provided by FBA under each gene overexpression allows us to evaluate its effect on biomass synthesis. Target genes identified based on the search algorithm are reactions and its corresponding genes which, upon overexpression, minimize byproduct synthesis and maximize biomass production efficiency (highest biomass yield on glucose, highest biomass produced per oxygen consumed). By examining the effect of single gene overexpression on biomass production, four target overexpressed genes were identified for maximizing biomass yield per glucose and oxygen uptake. The gene candidates are *GPD1* (Glycerol-3-phosphate dehydrogenase, R13r); *ZWF1* (Glucose 6-phosphate dehydrogenase, R15); *TKL1* (Transketolase, R18r/19r); and *CIT1* (Citrate synthase, R21/73) as summarized in Supplementary Figure S1 and Table S1. The designed mutants that render target gene overexpression are expected to reach a biomass yield of 0.49 g-cdw/g-glucose with a biomass production efficiency per oxygen uptake at 0.08 g-cdw/mmol-oxygen.

3.2. Construction of designed mutants

To verify the model prediction, mutants designed based on FBA were experimentally constructed based upon a non-homologous end joining recombination. Target overexpressed genes were integrated onto the chromosome by transforming wild-type strain with individual constructed integrative plasmid. Four single gene overexpression mutant strains SJU02 (GPD1 overexpression), SJU03 (TKL1 overexpression), SJU04 (CIT1 overexpression) and SJU05 (ZWF1 overexpression) were successfully constructed. The detailed genotype of the constructed strains is summarized in Table 1. DNA amplification with primers specified to the 5′-region of the overexpressed gene and *AOX1* terminator was undertaken to verify the presence of an extra copy of the target gene on the mutant's chromosome (Fig. 1). All expected DNA fragment sizes appeared for the mutants but were absent for the wild-type strain, thus confirming the construction of the gene overexpressed mutant. The wild-type was transformed with pTEF1:mZeo vector and used as control strain (SJU01) for cell growth comparison.

3.3. Strain characterization for biomass synthesis

To quantify biomass performance of the constructed mutants, we monitored the cell growth and fermentation profiles of SJU02, SJU03, SJU04 and SJU05 in comparison with the control SJU01 under an identical batch growth experiment. Fig. 2A–E shows the time profiles of glucose, cell growth and fermentation products during 24 hrs cultivation. In all cases, the mutants (SJU02, SJU03, SJU04 and SJU05) achieved higher biomass concentration than the control. Of the characterized strains, SJU05 (ZWF1 overexpression) exhibited the best performance with the highest final biomass titer of 9.81 ± 0.40 g-cdw/l, a 1.48-fold increase compared to a final biomass titer of 6.62 ± 0.22 g-cdw/l by the control. Although SJU03 and SJU04 attained higher biomass yield in batch growth experiments, they grew slower than the control (Fig. 2F). SJU04 had the slowest specific growth rate of 0.27 ± 0.01 hr^{-1} during exponential growth phase, an 18% reduction from the specific growth rate of 0.33 ± 0.01 hr^{-1} in the control. This change was accompanied by the reduction of glucose uptake rate in SJU04. In contrast, SJU05 grew slightly faster than the control. The designed mutants SJU02, SJU03, SJU04 and SJU05 exhibited biomass yield on glucose approximately 30%, 25%, 30% and 44% higher than that achieved by SJU01, respectively (Fig. 2F). In agreement with the model prediction, SJU05 apparently functions through the most efficient biosynthesis pathway producing biomass at a maximum yield of 0.49 g-cdw/g-glucose and achieves the highest biomass productivity of 0.78 g-cdw/l-hr. Other overexpressed mutants achieved 89% (SJU02), 86% (SJU03) and 90% (SJU04) of maximum predicted yield. The growth phenotypes of all strains are summarized in Table 2.

Fig. 3 compares the byproduct distribution of mutants and control strain showing ethanol as a major fermentative byproduct. This is expected since *S. stipitis* is known to be able to ferment sugar to ethanol at a relatively high yield. In all mutants, ethanol production was decreased in response to the increased biomass production. The control SJU01 exhibited ethanol accumulation at a yield of 0.28 ± 0.03 g-EtOH/g-glucose, which was higher than the yield achieved by SJU02, SJU03, SJU04 and SJU05 mutants at 0.12 ± 0.02, 0.22 ± 0.03, 0.07 ± 0.01 and 0.23 ± 0.00 g-EtOH/g-glc, respectively. The accumulated ethanol concentration after 24 hrs cultivation reached 46.2% of the total carbon for the control, 32.0% for SJU02, 39.9% for SJU03, 22.0% for SJU04 and 42.5% for SJU05.

3.4. Flux distribution comparison

Metabolic flux distribution of SJU02, SJU03, SJU04 and SJU05 mutants in comparison with SJU01 control strain was analyzed to

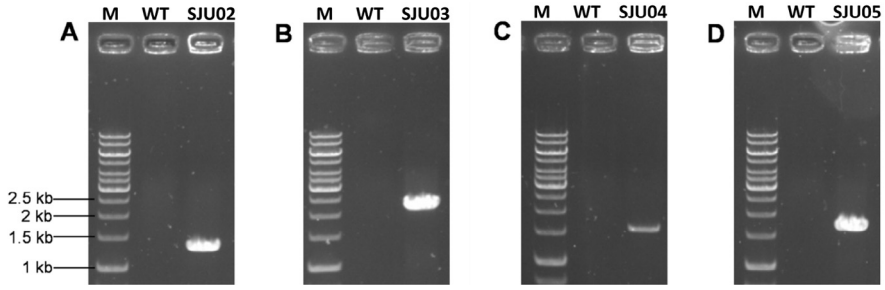

Fig. 1. The presence of overexpressed genes in the mutants confirmed by PCR using the sense and antisense primers corresponding to the 5′ region of target gene and *AOX1* terminator in expression plasmid (Supplementary Table S2). The amplified products in the mutant SJU02 (A), SJU03 (B), SJU04 (C) and SJU05 (D) in comparison with the wild-type. In each figure, 1 kb DNA marker is shown in lane M followed by amplified product of wild-type (WT) as negative control, and amplified product of mutant.

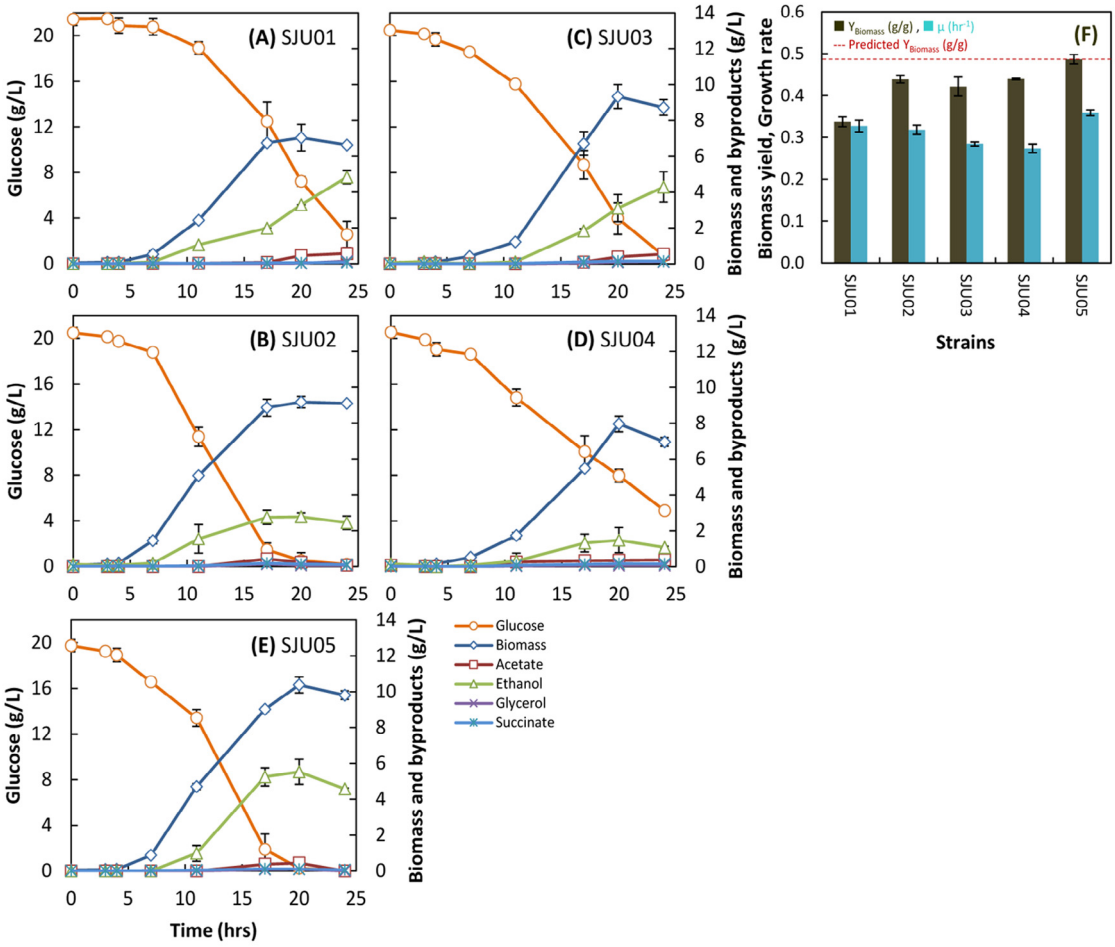

Fig. 2. Cell growth and fermentation kinetics of the controlled strain SJU01 (A) in comparison with gene overexpression mutants SJU02 (B), SJU03 (C), SJU04 (D), and SJU05 (E). Shown are time profiles for glucose concentration (○), biomass concentration (◇) and fermentative byproducts (□ acetate; △ ethanol; × glycerol: ✳ succinate). (F) Growth performance comparison for biomass yield and specific growth rate in mutants and control.

examine the changes in the central metabolism upon overexpression of target genes. These fluxes were determined from FBA using measured rates of glucose uptake, cell growth and ethanol formation as inputs for calculation. The measured biomass yield agrees well with the yield predicted by flux distribution analysis (Fig. 4A). Redox and ATP analysis reveal higher ATP and NADPH availability in SJU02, SJU03, SJU04 and SJU05 than the control (Fig. 4B). A 15–24% increase in ATP availability observed in the mutants suggests higher energy currency in the mutant metabolism compared to the control.

Table 2
Growth phenotype performance for the control SJU01, the mutants SJU02, SJU03, SJU04 and SJU05 and their evolved derivatives SJU02E, SJU03E, SJU04E.

Strains	Biomass (g/l)[a]	Biomass yield (g/g)[b]	Spec. growth rate (hr^{-1})[c]
SJU01	6.62 ± 0.22	0.34 ± 0.01	0.33 ± 0.01
SJU02	9.10 ± 0.10	0.44 ± 0.01	0.32 ± 0.01
SJU03	8.72 ± 0.43	0.42 ± 0.02	0.28 ± 0.00
SJU04	7.96 ± 0.24	0.44 ± 0.01	0.27 ± 0.01
SJU05	9.81 ± 0.40	0.49 ± 0.01	0.36 ± 0.01
SJU02E	10.03 ± 0.58	0.49 ± 0.03	0.34 ± 0.00
SJU03E	10.03 ± 0.67	0.49 ± 0.03	0.33 ± 0.00
SJU04E	9.91 ± 0.06	0.49 ± 0.01	0.34 ± 0.01

[a] Final biomass concentration is estimated final OD_{600nm} after 24 hrs aerobic cultivation using the following correlation, g-cdw/l = 0.359 × OD_{600nm}.
[b] Biomass yield is based on total biomass produced per total glucose consumed.
[c] Specific growth rate is calculated from the slope of the time plot of ln(OD_{600nm}).

The availability of NADPH was highest in the SJU05 mutant, indicating that overexpression of ZWF1 probably redirects cell metabolism to increase fluxes through the pentose phosphate pathway, which is known to be the main source of NADPH cofactor.

Comparative flux distribution of SJU02, SJU03, SJU04 and SJU05 mutants were based on flux ratio,[10] a ratio between expressed flux of the mutants and that of the control (Fig. 4C). All fluxes were normalized with glucose uptake rate. Flux ratio analysis identified upregulated reactions (flux ratio >>1) associated with the synthesis of biomass precursors, NADPH and ATP cofactors. A significant increase in fluxes toward the TCA cycle was observed in all mutants including the increase in R31r (Succinate dehydrogenase, SDH), R73 (Citrate synthase, CIT), R74r (Aconitate hydratase, ACO) and R80r (Fumarase, FUM), which could lead to an increase in several biosynthesis precursors such as α-ketoglutarate and oxaloacetate for amino acid and nucleotide synthesis. Rate of reaction R72 (Pyruvate dehydrogenase, PDH) was also increased in the mutants compared to the control, presumably to increase availability of acetyl-CoA, a key precursor for lipid and amino acid synthesis. It was also observed that the mutants lower flux toward R38 (Pyruvate decarboxylase, PDC) and R40 (Alcohol dehydrogenase, ADH), resulting in less ethanol being produced and more NADH availability for ATP synthesis. More fluxes to reaction R68 (O_2 transport) and R56 (Oxidative phosphorylation) in the mutant enhanced oxygen utilization and increased the generation of ATP used for biomass synthesis, respectively. This could result in more effective proton gradients and

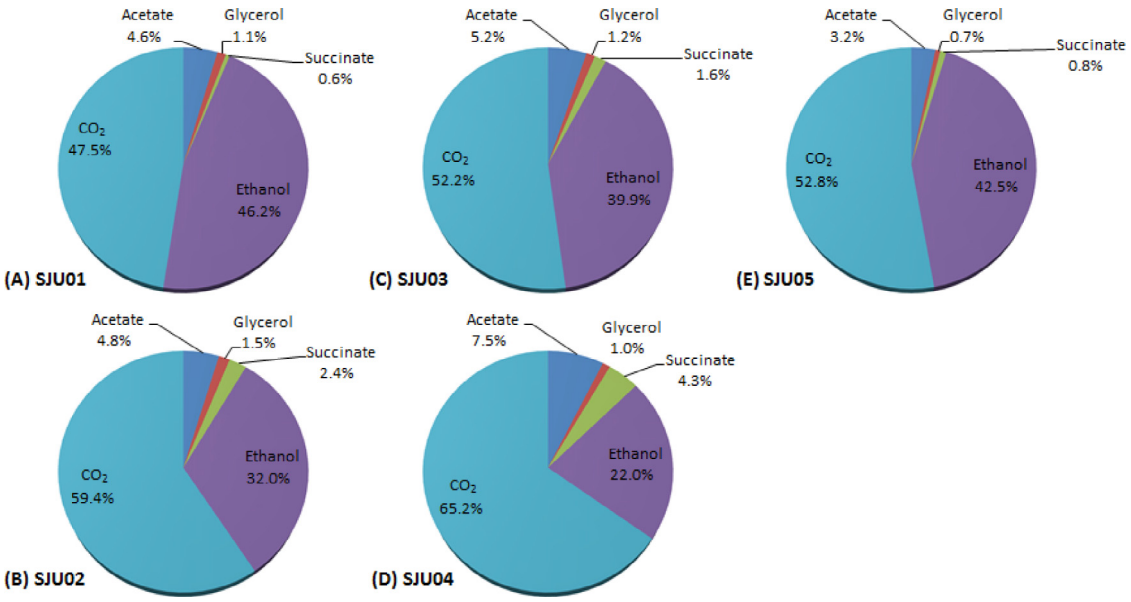

Fig. 3. Percent carbon distribution of byproducts for the control strain SJU01 (A) in comparison with gene overexpression mutants SJU02 (B), SJU03 (C), SJU04 (D), and SJU05 (E) in aerobic batch shake-flask culture. The percent distribution was calculated based on carbon mole concentration of byproducts secreted per carbon mole of glucose consumed after 24 hrs cultivation time. In order to compare carbon distribution among byproducts, biomass was excluded from the percent distribution calculation. The accumulated mole concentration of CO_2 was estimated based on the reaction stoichiometry of byproduct synthesis as follows: $[CO_2] = 2[Succ] + [EtOH] + 3[Gly] + [Acet] + 12.4[Bio]$.

consequently improve bioenergetic efficiency in the mutants. Thus, the mutants may be beneficial for biotechnology applications dealing with high cell density cultivations where the supply of oxygen becomes limiting.

Comparing the flux control coefficient (FCC) of each reaction in the metabolic network helps to identify major rate-controlling reaction for biomass synthesis in each mutant. Reactions R72 (Pyruvate dehydrogenase, PDA), R73 (Citrate synthase, CIT), R74r (Aconitate hydratase, ACO) and R80r (Fumarase, FUM) in the TCA pathway were identified as major limiting reactions in the metabolic network of mutant SJU02 based on high value of FCC (Fig. 4D). The FCC analysis also revealed R31r (Succinate dehydrogenase, SDH), R56

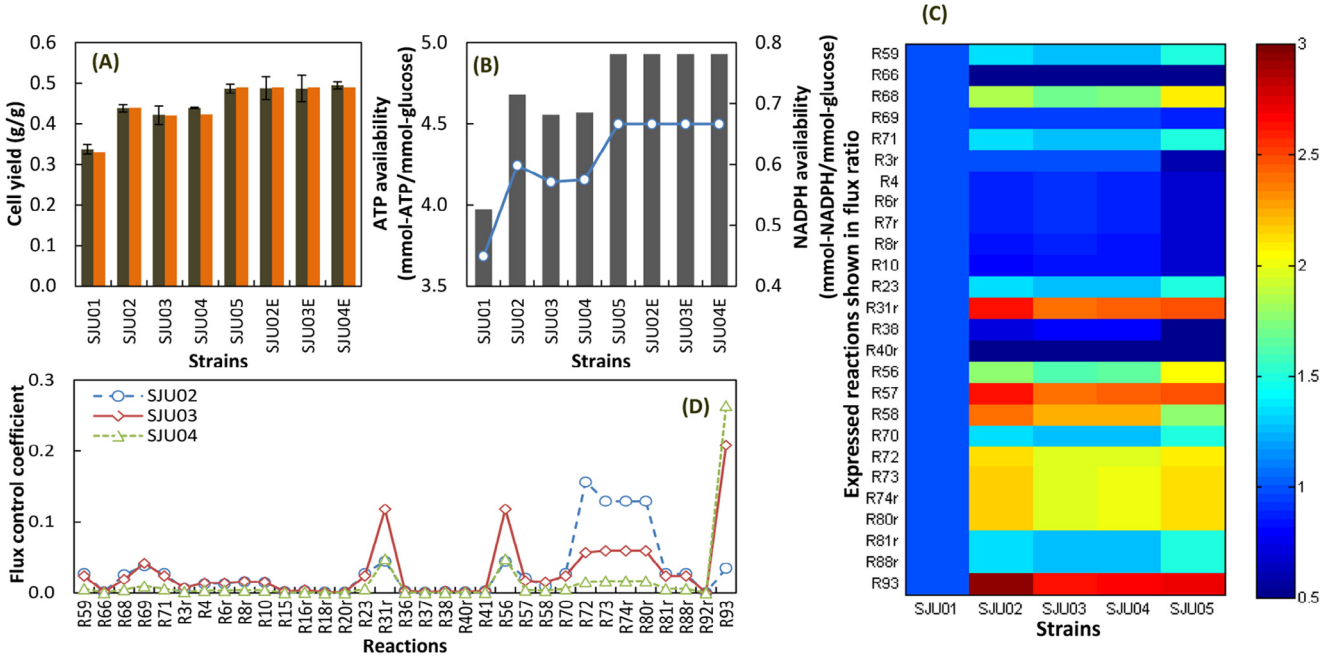

Fig. 4. (A) Measured and predicted biomass yield for gene overexpression mutants and their evolved derivatives in comparison with the control. Experimental yields (gray) of control SJU01, mutants SJU02, SJU03, SJU04, SJU05, and their evolved derivatives SJU02E, SJU03E, SJU04E are compared with the predicted yields (orange) based on flux distribution analysis of *S. stipitis* metabolic network model. (B) NADPH redox (blue circle) and ATP (gray bar) availability of different mutant strains in comparison with the control based on Eqs. 2 and 3. (C) Comparative flux expression of different strains of *S. stipitis*. Expressed flux in each reaction is given in flux ratio. Reaction names and their corresponding genes and enzymes are according to the names given in the previous metabolic model of *S. stipitis*.[14] Only fluxes with significant change when compared with control are considered. (D) Flux control analysis of the metabolic network of mutants SJU02, SJU03 and SJU04 based on Eq. 4.

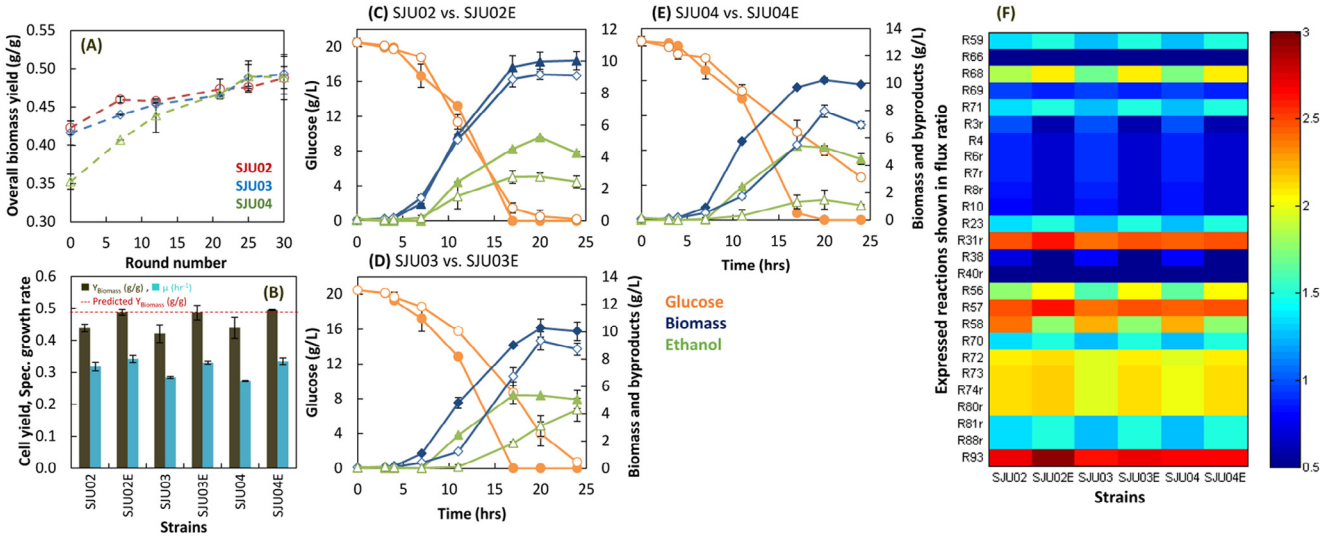

Fig. 5. (A) Dynamic changes in overall biomass yields of SJU02, SJU03 and SJU04 through metabolic evolution. The evolved strains were isolated and named SJU02E, SJU03E and SJU04E, respectively. (B) Growth performance comparison for biomass yield and specific growth rate in mutants and their evolved derivatives. Time profiles of cell growth, glucose consumption and ethanol secretion for mutants and their evolved derivatives. (C) Mutant SJU02 and evolved mutant SJU02E, (D) mutant SJU03 and evolved mutant SJU03E, and (E) mutant SJU04 and evolved mutant SJU04E under aerobic batch culture. Unevolved strains are shown in empty symbols, while the evolved strains are given in filled symbols. (F) Comparative flux expression of unevolved and evolved strains of *S. stipitis*. Expressed flux in each reaction is given in flux ratio, which is compared to that of the control strain SJU01. Reaction names and their corresponding genes and enzymes are according to the names given in the previous metabolic model of *S. stipitis*.[14] Only fluxes with significant change when compared with control are considered.

(Oxidative phosphorylation) and R93 (ADP/ATP mitochondrial transport) as reactions with high degree of control for biosynthesis in SJU03 and SJU04 mutants. It is expected that increasing fluxes through these rate-controlling reactions would, therefore, result in enhanced biomass synthesis. The results support this hypothesis since all reactions with high flux control coefficient were found to be up-regulated corresponding to increasing biomass production in the mutants (Fig. 4C). These reactions could also be targeted for optimization during metabolic evolution in order to further improve biomass production in the mutants.

3.5. *Metabolic evolution of the designed mutants*

A metabolic evolution experiment was performed for each mutant SJU02, SJU03 and SJU04. Evolved strains with increased biomass production are expected to emerge from the evolution process, since growth is used as selective pressure. The overall biomass yield of the evolving mutant in batch culture, which is based on total glucose added initially, was periodically monitored during the evolution. After 30 rounds of serial transfer, individual evolved strains were isolated and named after their parent as SJU02E, SJU03E and SJU04E, respectively. Fig. 5A shows changes in overall biomass yield of SJU02, SJU03 and SJU04 during the evolution process. The overall yield continued to increase with the number of transfers and reached a plateau after 25 rounds of serial dilution culture. The continuous increase in biomass yield with number of transfers is presumably a result of evolved strains with better cell growth emerging and successively replacing the parental strains. All evolved mutants converged to the same biomass yield during the course of evolution (Fig. 5A). The evolved derivatives exhibited biomass yields of 0.49 ± 0.03 g-cdw/g-glucose for SJU02E, 0.49 ± 0.03 g-cdw/g-glucose for SJU03E and 0.49 ± 0.01 g-cdw/g-glucose for SJU04E, which is the maximum predicted yield based on FBA (Fig. 5B). This is equivalent to approximately 11–16% improvement in biomass yield compared to the corresponding parent strain(s) and 44% improvement compared to SJU01. The evolved mutants also grew faster at about 10–22% higher specific growth rates than their parents and produced biomass at a higher rate, 0.76 g/l-hr in SJU02E, 0.71 g/l-hr in SJU03E, 0.72 g/l-hr in SJU04E, compared to 0.52 g/l-hr in SJU01 and reached similar biomass titer, higher than their parents (Fig. 5C–E). Furthermore, evolved strains exhibited remarkable improvements in glucose utilization rates, especially for SJU03E and SJU04E. It took the parent strains about 24 hrs or longer to consume 20 g/l of glucose, while evolved mutants completed all glucose at around 17–20 hrs. The growth phenotypes of evolved mutants are summarized in Table 2.

Comparative flux distribution analysis reveals the readjustment of the mutant metabolism toward efficient biomass formation by increasing fluxes in major rate-limiting reactions during metabolic evolution (Fig. 5F). In the evolved mutants, rate-controlling fluxes R73 (Citrate synthase, CIT), R74r (Aconitate hydratase, ACO) and R80r (Fumarase, FUM) in the TCA pathway increased by 7%. The 7% and 9% increase in fluxes through R31r (Succinate dehydrogenase, SDH) and R93 (ADP/ATP mitochondrial transport) respectively was also observed during evolution. Reaction R72 (Pyruvate dehydrogenase, PDA), a NADH-synthesizing reaction, was also increased in the evolved strains, likely to redirect fluxes toward biomass precursors in pyruvate metabolism and TCA cycle. The increase in R56 (Oxidative phosphorylation) was more pronounced than any other fluxes, 15–25%, which is by far the most significant flux change obtained in the evolved mutants. Elevating fluxes in R56/R93 reactions also lead to increasing availability of ATP for biosynthesis, hence improving biomass yield. Additionally, the improved biomass in evolved strains may be associated with increasing NADPH cofactor supply (Fig. 4B).

4. Discussion

We present, in this study, a systematic approach for engineering efficient cell factory using systems metabolic engineering guided by FBA in conjunction with metabolic evolution. This combinatorial strategy was applied for optimizing biomass synthesis in *S. stipitis* growing on glucose. Systems metabolic engineering based on FBA was utilized to design mutants capable of operating according to

the most efficient biomass synthesis pathway. Four mutant candidates were theoretically identified by FBA and experimentally constructed. The metabolic evolution was later applied for fine-tuning the metabolism of the designed strains.

As a consequence of overexpressing target genes, the metabolism of the designed mutants was readjusted toward an efficient biosynthesis pathway by increasing the availability of biomass precursors and cofactors. The decreased ethanol secretion in the mutants is expected as a result of more carbon flux utilized for biomass and less for ethanol. Less ethanol production in the mutants also increases NADH supply and consequently increases ATP availability for biomass since ethanol primarily serves as an electron sink for NADH drainage (Fig. 4B,C). A slight increase in glycerol secretion was observed in the GPD1 overexpressed mutant (SJU02) as GPD1 is a reversible part of the glycerol synthesis pathway. A similar trend is observed in *S. cerevisiae* with GPD1 overexpression.[2,20,21] Increased CO_2 production in the mutants (Fig. 3) corresponds to increased activity in the TCA cycle (Fig. 4C) since this pathway is one of the major paths for CO_2 generation. The mutant with CIT1 overexpression (SJU04) reveals an increased level of succinate due to elevated fluxes in the TCA cycle as CIT1 is the first step of the pathway. This observation also agrees well with a previous experiment.[22]

It is interesting to note that the ZWF1 overexpressed mutant (SJU05) secreted acetate at a reduced amount when compared to the control and other mutants. The acetate synthesis pathway can be utilized as an alternative path for supplying NADPH since every mole of acetate produced generates one mole of NAD(P)H via aldehyde dehydrogenase, which is then used for synthesis of biomass precursors. The ZWF1 overexpressed mutant may take an alternative route for NADPH generation likely through the pentose phosphate pathway, leading to less carbon loss in the form of acetate and more carbon available for biosynthesis. A previous study shows that the ZWF1 gene accounts for 35–55% of the total NADPH pool generated in the cell metabolism.[23] Hence, increased biomass yield in SJU05 may be partially corresponding to increasing NADPH supply as demonstrated in flux distribution analysis (Fig. 4B).

Increasing fluxes through the TCA cycle in all mutants (Fig. 4C) replenishes the NADH pool for biosynthesis, leading to improved biomass production. Elevated flux through R58, an NAD-NADH mitochondrial transporter, likely permits an efficient exchange of cofactors between cytosol and mitochondria in order to sufficiently supply the cofactors required for biosynthesis in cytosol. Concomitantly, increased flux through R93 (ADP/ATP mitochondrial transport) allows more ATP availability for biosynthesis in the mutants by facilitating the exchange of ATP between the cytosol and mitochondria. All the evidence suggests that a limiting factor for producing biomass at high yield could be a high demand of ATP and NADPH which cannot be met in wild-type metabolism.

Although SJU02, SJU03 and SJU04 achieved higher biomass yield on glucose than the control, they apparently did not operate according to the maximum predicted yield. The discrepancy between measured and predicted yield suggests that the mutants may be subjected to local control of rate-limiting reactions with low enzyme capacities within the cell metabolic pathway, therefore, preventing them from achieving the maximum yield. The enzyme capacities in rate-limiting reactions could be manipulated naturally through a directed evolution of cell metabolism with selection of cells having improved cell growth. This metabolic evolution strategy has been previously proven to be a successful strategy to liberate the control of rate-limiting enzymes for enhancing cell capacities.[24–27] Using the metabolic evolution approach, the biomass yield of the evolved derivatives matched closely with the predicted yield (Fig. 4A), suggesting that a cell evolves by readjusting its metabolic flux distribution toward the computationally predicted growth phenotype. This finding is in agreement with previous studies showing that the metabolism of an evolving cell can be predicted by FBA.[28,29] Improvement in cell growth and substrate utilization during evolution is also commonly observed in previous studies.[28,30] The evolved mutants exhibited an interesting phenotype in byproducts synthesis showing higher ethanol production, whereas secretion of acetate, glycerol and succinate was lower compared to their parent (Fig. 5C–E). The evolution mechanism of a cell to enhance its metabolic capacity by increasing rate-controlling fluxes within metabolic network as shown in Figs. 4D and 5F is also previously reported in several studies.[27,31,32] Identification of mutations occurring during the evolution could be achieved through methods such as comparative genome sequencing or transcriptome analysis, which is left for future investigation.

4.1. Conclusion

All data indicate that *S. stipitis* mutants (SJU02E, SJU03E, SJU04E and SJU05) operated according to the efficient biomass producing pathway that was predicted by FBA and optimized through metabolic evolution. This study proves systems metabolic engineering guided by FBA together with metabolic evolution as a powerful combinatorial approach for rational design of an efficient cell factory. The strains developed in this study could possibly be used as platform host for high-cell-density fermentations as well as for metabolic engineering of other foreign pathways for both growth- and non-growth associated products that require precursors and cofactors similar to the biosynthesis pathway.

Acknowledgements

This work has been supported by Platform Technology grant from National Center for Genetic Engineering and Biotechnology, Thailand (No. P-13-50084). The authors would like to thank Dr. Niran Roongsawang for kindly providing CBS6054 strain and pTEF1:mZeo vector used for gene overexpression plasmid construction. Author contributions: P.U. planned the research study, constructed the model, performed the analysis, interpreted the results and wrote the paper. S.J. planned the research study, constructed the mutants, interpreted the results and wrote the paper. K.L. revised the paper. All authors approved the final version of the paper.

This article does not contain any studies with human participants or animals performed by any of the authors. The authors declare no commercial or financial conflict of interest.

Appendix: Supplementary material

Supplementary data to this article can be found online at doi:10.1016/j.synbio.2016.01.006.

References

1. Shi J, Zhang M, Zhang L, Wang P, Jiang L, Deng H. Xylose-fermenting *Pichia stipitis* by genome shuffling for improved ethanol production. *Microb Biotechnol* 2014;**7**(2):90–9.
2. Yao Y, Yang L, Kun-Tao P, Tan H, Ying-Fang N, Wei-Hong X, et al. Glycerol and neutral lipid production in the oleaginous marine diatom *Phaeodactylum tricornutum* promoted by overexpression of glycerol-3-phosphate dehydrogenase. *Biotechnol Biofuels* 2014;**7**:110–9.
3. Lee JW, Kim TY, Jang YS, Choi S, Lee SY. Systems metabolic engineering for chemicals and materials. *Trends Biotechnol* 2011a;**29**(8):370–8.
4. Lee JW, Na D, Park JM, Lee J, Choi S, Lee SY. Systems metabolic engineering of microorganisms for natural and non-natural chemicals. *Nat Chem Biol* 2012;**8**(6):536–46.
5. Toya Y, Shimizu H. Flux analysis and metabolomics for systematic metabolic engineering of microorganisms. *Biotechnol Adv* 2013;**31**(6):818–26.
6. Lee JW, Zhu JY, Scordia D, Jeffries TW. Evaluation of ethanol production from corncob using *Scheffersomyces (Pichia) stipitis* CBS 6054 by volumetric scale-up. *Appl Biochem Biotechnol* 2011b;**165**:814–22.

7. Antoniewicz MR. Methods and advances in metabolic flux analysis: a mini-review. *J Ind Microbiol Biotechnol* 2015;**42**(3):317–25.
8. Price ND, Reed JL, Palsson BO. Genome-scale models of microbial cells: Evaluating the consequences of constraints. *Nat Rev Microbiol* 2004;**2**(11):886–97.
9. Trinh CT, Thompson RA. Elementary mode analysis: a useful metabolic pathway analysis tool for reprograming microbial metabolic pathways. *Subcell Biochem* 2012;**64**:21–42.
10. Unrean P, Franzen CJ. Dynamic flux balance model of *S. cerevisiae* for elucidation of cellular response to furfural perturbation. *Biotechnol J* 2015;**10**(8):1248–58.
11. Fong SS, Burgard AP, Herring CD, Knight EM, Blattner FR, Maranas CD, et al. *In silico* design and adaptive evolution of *Escherichia coli* for production of lactic acid. *Biotechnol Bioeng* 2005a;**91**(5):643–8.
12. Agren R, Otero JM, Nielsen J. Genome-scale modeling enables metabolic engineering of *Saccharomyces cerevisiae* for succinic acid production. *J Ind Microbiol Biotechnol* 2013;**40**(7):735–47.
13. Alper H, Jin YS, Moxley JF, Stephanopoulos G. Identifying gene targets for the metabolic engineering of lycopene biosynthesis in *Escherichia coli*. *Metab Eng* 2005;**7**(3):155–64.
14. Unrean P, Nguyen NH. Metabolic pathway analysis of *Scheffersomyces stipitis*: effect of oxygen availability on ethanol synthesis and flux distributions. *Appl Microbiol Biotechnol* 2012;**94**:1387–98.
15. Puseenam A, Tanapongpipat S, Roongsawang N. Co-expression of endoxylanase and endoglucanase in Scheffersomyces stipitis and its application in ethanol production. *Appl Biochem Biotechnol* 2015;doi:10.1007/s12010-015-1846-1.
16. Thompson JR, Register E, Curotto J, Kurtz M, Kelly R. An improved protocol for the preparation of yeast cells for transformation by electroporation. *Yeast* 1998;**14**:565–71.
17. Hanly TJ, Urello M, Henson MA. Dynamic flux balance modeling of *S. cerevisiae* and *E. coli* co-cultures for efficient consumption of glucose/xylose mixtures. *Appl Microbiol Biotechnol* 2012;**93**:2529–41.
18. Heinrich R, Schuster S. The modelling of metabolic systems: structure, control and optimality. *Biosystems* 1998;**47**(1):61–77.
19. Rutkis R, Kalnenieks U, Stalidzans E, Fell DA. Kinetic modelling of the *Zymomonas mobilis* Entner-Doudoroff pathway: insights into control and functionality. *Microbiology* 2013;**159**:2674–89.
20. Varela C, Kutyna DR, Solomon MR, Black CA, Borneman A, Henschke PA, et al. Evaluation of gene modification strategies for the development of low-alcohol-wine yeasts. *Appl Environ Microbiol* 2012;**78**(17):6068–77.
21. Remize F, Barnavon L, Dequin S. Glycerol export and glycerol-3-phosphate dehydrogenase, but not glycerol phosphatase, are rate limiting for glycerol production in *Saccharomyces cerevisiae*. *Metab Eng* 2001;**3**(4):301–12.
22. Lin AP, Anderson SL, Minard KI, McAlister-Henn L. Effects of excess succinate and retrograde control of metabolite accumulation in yeast tricarboxylic cycle mutants. *J Biol Chem* 2011;**286**(39):33737–46.
23. Minard KI, McAlister-Henn L. Sources of NADPH in yeast vary with carbon source. *J Biol Chem* 2005;**280**(48):39890–6.
24. McKenna R, Thompson B, Pugh S, Nielsen DR. Rational and combinatorial approaches to engineering styrene production by *Saccharomyces cerevisiae*. *Microb Cell Fact* 2014;**13**:123–35.
25. Otero JM, Cimini D, Patil KR, Poulsen SG, Olsson L, Nielsen J. Industrial systems biology of *Saccharomyces cerevisiae* enables novel succinic acid cell factory. *PLoS ONE* 2013;**8**(1):e54144.
26. Lee SM, Jellison T, Alper HS. Systematic and evolutionary engineering of a xylose isomerase-based pathway in *Saccharomyces cerevisiae* for efficient conversion yields. *Biotechnol Biofuels* 2014;**7**(1):122–30.
27. Rohlin L, Oh MK, Liao JC. Microbial pathway engineering for industrial processes: evolution, combinatorial biosynthesis and rational design. *Curr Opin Microbiol* 2001;**4**(3):330–5.
28. Fong SS, Palsson BØ. Metabolic gene-deletion strains of *Escherichia coli* evolve to computationally predicted growth phenotypes. *Nat Genet* 2004;**36**(10):1056–8.
29. Fong SS, Joyce AR, Palsson BØ. Parallel adaptive evolution cultures of *Escherichia coli* lead to convergent growth phenotypes with different gene expression states. *Genome Res* 2005b;**15**(10):1365–72.
30. Hua Q, Joyce AR, Fong SS, Palsson BØ. Metabolic analysis of adaptive evolution for in silico-designed lactate-producing strains. *Biotechnol Bioeng* 2006;**95**(5):992–1002.
31. Flowers JM, Sezgin E, Kumagai S, Duvernell DD, Matzkin LM, Schmidt PS, et al. Adaptive evolution of metabolic pathways in Drosophila. *Mol Biol Evol* 2007;**24**(6):1347–54.
32. Olson-Manning CF, Lee CR, Rausher MD, Mitchell-Olds T. Evolution of flux control in the glucosinolate pathway in *Arabidopsis thaliana*. *Mol Biol Evol* 2013;**30**(1):14–23.